

# Heat Transfer Analysis in Sound-Enhanced Fluidized Beds Containing Geldart B-C Binary Mixtures

Mohitkumar G. Gabhane<sup>1\*</sup>, Siddharth S. Chakrabarti<sup>2</sup>, Uday S. Wankhede<sup>3</sup>

<sup>1</sup>Research Scholar, Mechanical Engineering Department, School of Engineering, OP Jindal University, Punjipathra, Raigarh, India; E-mail: [mohitgabhane79@gmail.com](mailto:mohitgabhane79@gmail.com)

<sup>2</sup>Professor, Mechanical Engineering Department, School of Engineering, OP Jindal University, Punjipathra, Raigarh, India

<sup>3</sup>Associate Professor, Mechanical Engineering Department, Government College of Engineering, Nagpur, Maharashtra, India

**Abstracts:** An experimental study was carried out on the binary mixing behaviour of Group C with Group B particles as well as the heat transfer behaviour between the bed and submerged heating tube in an acoustic field. The effects of excessive air velocity, sound pressure intensity, and local and averaged heat transfer coefficient were studied for five binary mixes. Different binary mixture fluidization ratios with and without sound aid are used to compare the results. The study also discusses the measurement techniques used, including pressure measurements and the characteristics of the bed solids. Sand and hydrophilic bituminous coal are used as the binary mixture materials, with different proportions of each. The experiments are conducted both with and without acoustic assistance to compare the outcomes. This study provides insights into the heat transfer behavior and binary mixing in a sound-assisted fluidized bed. The findings indicate that sound assistance has a significant impact on the heat transfer performance of Geldart B-C binary mixtures in fluidized beds. It highlights the potential benefits of using acoustic energy to improve fluidization quality in binary systems.

**Keywords:** Heat Transfer in Fluidized Bed, Binary Mixing Behaviour, Acoustic Energy, Mixing Strength.

## 1. INTRODUCTION

Fluidized beds are favored due to their high mixing strength and exceptional characteristics (Bai and Si 2020), fast segregation (Freitas et al. 2017), massive material handling capacity (Tang et al. 2019), constant temperature and particle size distribution (Leckner, Szentannai, and Winter 2011), and optimal mass / heat transfer rate (Abdelmotalib et al. 2015). Due to their good gas-solid contacting and largely regular temperature profiles inside the beds, gas-solid fluidized beds have been extensively employed in both the chemical reaction and the physical operation process (Chang, Yang, and Zhang 2011). Fluidized systems operate on the basic principle that if flow through a bed made up of nanoparticles at a velocity greater than the settling velocity and equal to the minimum fluidization velocity ( $U_{mf}$ ), the bed of nanoparticles becomes partially suspended in the incoming flow (Gohel, Baldaniya, and Barot 2007). The resulting mixture of solids and gases seems to have the properties of a liquid, which is referred to as fluidization (Geldart 1973). However, fluidization takes into interpretation inter-particle forces, particle acceleration, fluid density, and agglomerate dimensions (Valverde and Castellanos 2008). Some studies select materials based on their density and mean particle size to suggest fluidization (Hamam et al. 2020). Pressure drop (Dong et al. 2013), bed expansion (Kim et al. 2017), contact distance (Hamidipour et al. 2005), bubble frequency (Ali et al. 2016), and particle travel distance (Nimvari, Zarghami, and Rashtchian 2020) all rise with increasing gas velocities, whereas the dead zone in fluidization and contact frequency fall (Wang et al. 2020). Enlarged dominant bubbles were observed at lower velocities, while spontaneous bubbling appeared at higher velocities (Hamidipour et al. 2005).

Numerous scholarly investigations have been conducted to examine the phenomenon of heat transfer in fluidized beds. In various industrial processes, such as gasification, combustion, drying, metallurgy, and heat treatment, the efficient exchange of thermal energy between the bed and heating tube plays a pivotal role (Wey, Lin, and You 2007). Sound vibrations increase gas molecule oscillation and cause them to overcome particle inertia, which utilized to breaks agglomerates continuously (Shrestha et al. 2020). While sound frequency is vital for acoustic fluidization, fluidization may not always grow monotonically with sound frequency (Chirone et al. 2018).

The addition of guest particles in varied amounts has been seen as a means to enhance the efficacy of nanoparticles (Han 2015). One of the best ways to increase fluidization effectiveness and minimize pressure decreases in fluidized beds is to use an acoustic field (Al- Ghurabi et al. 2019). Additionally, the acoustic field aids in the dissolution of electrostatic, liquid bridging, and intermolecular interactions. (Ali et al. 2016).

Material qualities, as well as frequency and sound pressure level, are significant factors determining fluidization effectiveness (Xiang et al. 2017). The impact of parameters such as particle diameter, tube diameter, system pressure, angular positions, and particle mixing on heat transfer has been studied and reported. Notably, there have been a few studies on fluidization of binary mixtures (Kang et al. 2017). Binary particle fluidization is more complicated than single-material fluidization, creating ample possibility for advancement (Raganati, Chirone, and Ammendola 2017). Untouched regions, such as binary mixtures of Geldart materials, can solve channeling and agglomeration issues. (Vaidya, Sonolikar, and Thombre 2013). Firing this binary mixture with a conventional furnace causes issues due to melted ash (Gabhane, Chakrabarti, and Wankhede 2021). Fluidized beds are employed to solve difficulties by mixing silica with bituminous coal powder. Silica sand is used in a fluidized bed to catch the flying away unburnt gas to give enough time to complete combustion and distribute heat evenly (Gabhane and Wankhede 2017).

The effects of the sound intervention on the fluidization of binary mixtures and the rate of heat transfer in fluidized beds have not yet been investigated in detail. This paper investigated heat transfer in a fluidized bed with sound assistance using a binary mixture in various ratios. Different binary mixing proportions with and without sound aid are used to compare the outcomes. Investigations were done into how sound assistance affected bed expansion, minimum fluidization velocity, and local and average heat transfer rates.

## 2. INSTRUMENTATION AND APPARATUS

### 2.1. Heat Transfer Facilities with A Fluidized Bed

Figure 1 shows the test column used for the experiments, which contained a horizontal heating element, a sound wave production device, and a cylindrical fluidizing column. A mild steel porous plate serves as a distributor for the fluidized bed with 100 mm inner diameter acrylic column, 500 mm height, 57 holes that are 0.5 mm square in pitch, and 5% frictional open pocket. A wind box (plastic chamber) that is 300 mm high was employed to guarantee uniform air dispersion. Above the distribution plate, 36-micron stainless steel mesh was installed to stop material from falling down into the wind box. A connected millimeter ruler was used to determine the bed's depth. The air from a compressor was utilized as the fluidizing gas. The flow rate of air is controlled and tested using a Rotameter of 100 LPM capacity with 5 manual regulator valve. The moisture content in the compressed gas was eliminated using the moisture separator. To achieve the desired temperature, a horizontal copper heating element of 90 mm in length was employed. Teflon bushes that support the heating element also reduce axial heat loss. To determine the provided heat flux, a voltmeter and Ammeter were also employed. A compressed air bypass line is additionally accessible.

The experiments were carried out at room temperature and atmospheric pressure. In order to record exact temperatures on the diameter of the heated tube at various places along the tube at four distinct sites at an angle of 90 °C to one another, as illustrated in figure 2. One thermocouple, positioned 2.5 cm from the bed's centre, was used to measure the temperature of the bed. The thermocouples were calibrated before the experiment started. The convective heat transfer coefficient was calculated using the following equation:

$$Q = V \times I / (A_{rod} \times (T_s - T_b)) \quad (1)$$

The  $h$  and  $V$  stand for the voltage in Watts and the convective heat transfer coefficient in  $W/m^2K$ , respectively.  $A$  stands for current in amps,  $A_{rod}$  for the area of the heating element,  $T_s$  for the surface temperature of the heating element at absolute zero, and  $T_b$  for the temperature of the bed. By countering the effect of agglomeration, enhancing fluidization with sound to achieve higher performance with low fluidization velocity. a sound-generation system, a data collection system, and a sound wave generator at the top of the free-board, together with a digital

signal generator, woofer, sound amplifier, and microphone for SPL measurements.

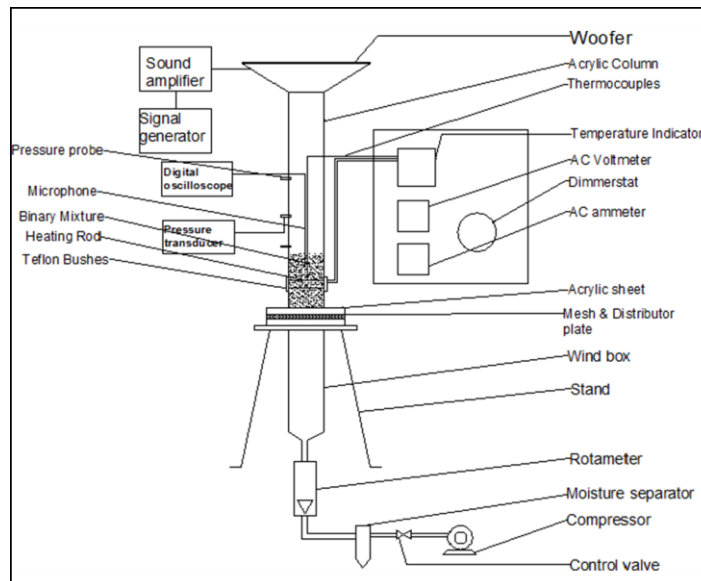


**Figure 1.** Schematic of the test rig

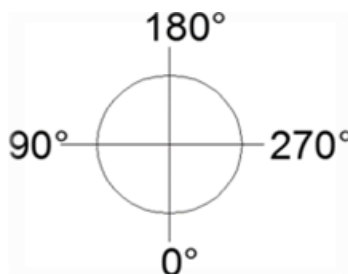
## 2.2. Measurement Technique

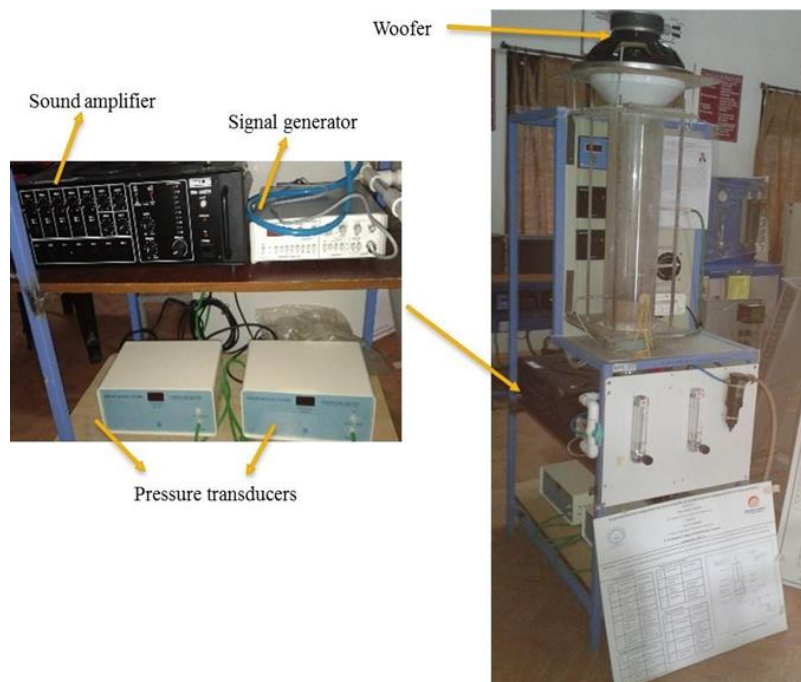
### a. Pressure Measurements

The pressure drop across the bed was calculated using an Arcanum Electronics optical pressure transducer in both static and dynamic circumstances. Differential pressure was recorded 20 mm below the gas distributor and at 5 cm, 10 cm, and 20 cm above the static bed along the test section. The compressor of 3 hp, 550 RPM produces maximum 10 bar pressure via moisture separator where the average bed depth was held mainly at 10 cm. To stop material transportation, pressure tap openings are aligned with the column wall and covered with filter tape.

### b. Bed Solids

Two separate materials in five different mixture proportions were used in this study. Sand with a mean diameter of 250 microns and an apparent density of  $1680 \text{ kg/m}^3$  was used which is the most common and extensively used fluidized material in the fluidized bed heat exchanger in Geldart B form. As a fluidizing material, hydrophilic bituminous coal (30% volatile matter + 20% ash + 3% moisture + 1% Sulphur + 0.2% Phosphorous + 45.8% Fixed carbon) was used. The primary particle size of this Geldart C substance is 20 microns. Its true density was around  $1346 \text{ kg/m}^3$ . The powder has a voidage of 98 percent overall. This kind of particle was commonly used as bed material in fluidized bed boilers. These materials were grouped in 50- 50, 25-75, and 75-25 percent mixtures, respectively. This would also aid in understanding the impact of each material particle's sovereignty on another. In addition to bed material, the superficial gas velocity, bed temperature, and sound intensities were all varied during the experiments.



**Figure 2.** Locations of thermocouples for radial temperature across the circumference of the heating rod**Figure 3.** Experimental setup

Our experimental strategy is split into two sections. The first section investigated the unassisted heat transfer of single and binary materials using varying superficial air velocities. Above a mean excessive air velocity of 9.6 cm/s, bed particle transportation was observed. We also looked at the SEM image after each experiment to get a deeper view of the agglomerates phenomena. The experiment was carried out in the second section by incorporating acoustic energy into fluidization at a frequency of 90 Hz with an intensity range of 110 dB to 144 dB. Before the binary mixture trials, the particles were put together in the fluidizing column, and the mixture was homogenized by airflow, as indicated by Ali and Asif (Ali and Asif 2017). After establishing bed homogeneity, the bed was allowed to settle down for a complete set.

Despite differences in particle size and density, the bed was evenly distributed. Table 1 summarizes the test conditions for measuring the heat transfer of various powders and mixtures.

### 3. HEAT TRANSFER FOR SAND AND BITUMINOUS COAL

Experiments were carried out to measure the local heat transfer coefficient at various positions around the circumference of the heated tube, as well as the overall heat transfer coefficient for various gas velocities, acoustic conditions, bed heights, and surface temperatures.

#### 3.1. Acoustic frequency for a fluidized bed with sound assistance

The correlation between sound pressure level (SPL) at the distributor and acoustic frequency is clearly demonstrated in Figure 4. The graph provides evident indication that the sound pressure level (SPL) reached its maximum value at a frequency of 90 Hz. Taking this into consideration, it may be inferred that sound waves exhibiting higher Sound Pressure Level (SPL) values at the free surface will also exhibit higher SPL values within the fluidized bed column. In order to achieve the highest Sound Pressure Level (SPL) within the fluidized bed, an experimental acoustic frequency of 90 Hz was employed.

**Table 1. description of the test conditions for measuring heat transfer**

Bed material	dp ( $\mu\text{m}$ )	Acoustic Condition	
		Acoustic frequency (Hz)	SPL (dB)
Coal	20	90	110, 120, 130, 140, 144, without sound
75% coal + 25% sand	78	90	110, 120, 130, 140, 144, without sound
50% coal + 50% sand	135	90	110, 120, 130, 140, 144, without sound
25% coal + 75% sand	192	90	110, 120, 130, 140, 144, without sound
Sand	250	90	110, 120, 130, 140, 144, without sound

**3.2. Bed temperature and acoustic frequency**

To assess the impacts of acoustic frequency on bed temperature, cold fluidization was performed and the temperature was measured using four thermocouples parallel to the heat-transmitting surface. Figure 5 shows variations in temperature at different acoustic frequencies. It was found that bed temperature increases slightly (0.5-0.7 °C). Hence, we consider a 90 Hz constant acoustic frequency for all the experiments conducted.

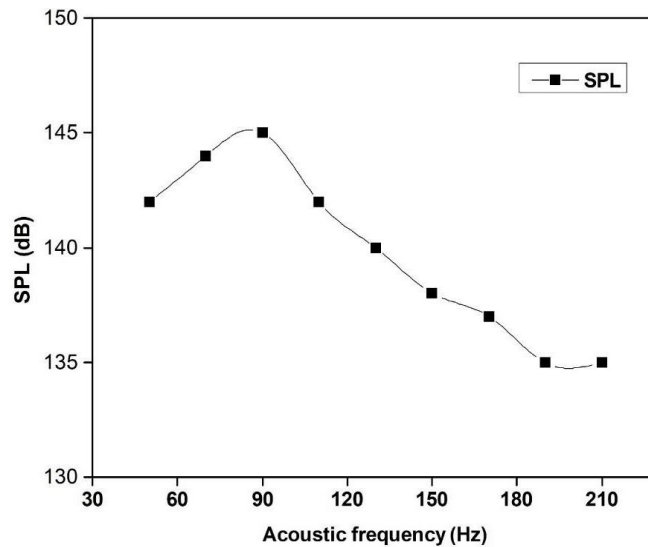


**Figure 4.** Deviation of SPL at distributor by acoustic frequency

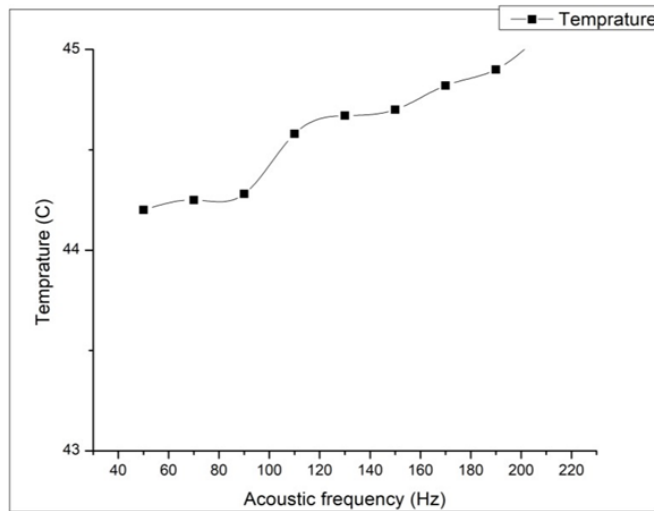


**Figure 5.** Temperature variation with acoustic frequency

### 3.3. Variation in Surface Temperature as A Function of Angular Orientation Along the Tube's Diameter

The local heat transfer coefficients variation in a heater tube with different fluid velocities and particle sizes can be seen in Figure 6. In the majority of cases, the highest temperatures were measured at the top ends of the tubes, i.e. sides that were perpendicular to the fluid flow. Because of the existence of gas bubbles at the top, the overall material circulation was detected at 90° and 270° of the tube, and the material concentration on the upstream side was significantly lower. It was also revealed that when the SPL increases, the temperature of the tube decreases. This is because the unpredictability in the fluidizing zone has increased, facilitating heat transmission.

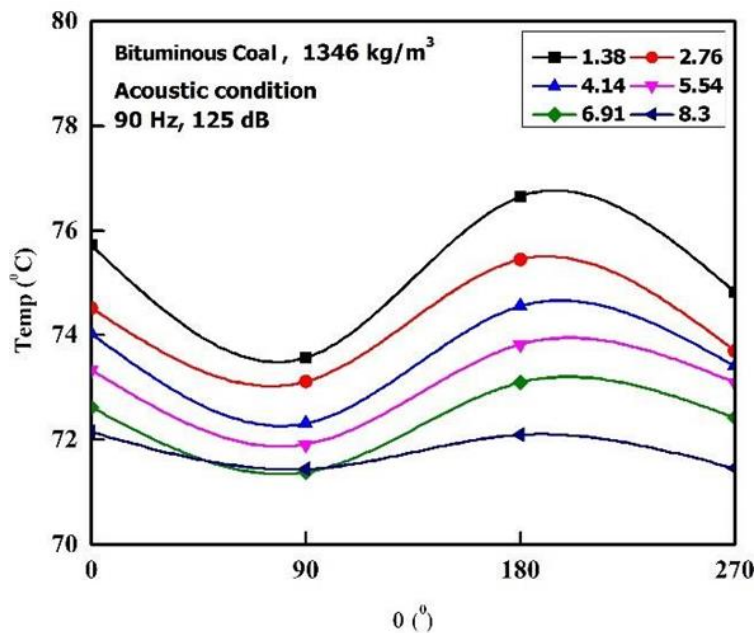


**Figure 6.** Surface temperature variation as a component of angular location along the diameter of a tube for bituminous coal, Q=8 W, L/D=1, 125dB, 90 Hz

### 3.4. Local Convective Heat Transfer Coefficient and Gas Velocity

The local heat transfer coefficient was independent of air velocity. The local heat transfer coefficient increases with increasing gas velocity due to the faster renewable of particle packets. Figure 7 illustrates the variations of the

local heat transfer coefficient for bituminous coal with excessive air velocity at varying values of  $\Theta$ . The study revealed that the augmentation in the heat transfer coefficient for coal is not substantial until an extra air velocity of 1.38 cm/s is reached. Nevertheless, the heat transfer coefficient exhibits an inclination to surpass the excessive air velocity of 2.76 cm/s. Heat transfer reaches its highest at an excessive velocity of 5.54 cm/sec. Three distinct particle motions have been observed along the tube's circumference; Stationary with no particle movement, particle sliding around the surface of the tube, and emulsion and bubbling phase mixing at high velocity (Wankhede and Sonolikar 2017). At the interface of mixing and sliding motion, highest values of heat transfer coefficient are observed.

Figure 8 shows how angular locations affect the local heat transfer coefficient for dissimilar readings of excessive air velocity ( $u_g - u_{mf}$ ) for sand ( $1680 \text{ kg/m}^3$ ). The local heat transfer coefficient was found to be highest at the 90° location on the tube's circumference. Larger heat transfer coefficients can be achieved by reducing the resident time of material packets with higher solid holdups. Heat transfer coefficients are higher at the top of the tube ( $180^\circ$ ) leading to a brief resident time of vigorous bubbling at a high frequency despite a smaller emulsion factor and solid hold-ups. Heat transfer after tube towards bed is intrinsically linked to particle motion caused by the bubbles. The change in surface temperature at  $\Theta = 180^\circ$  is influenced by bubble motion as well as particle sliding motion at the  $\Theta = 90^\circ$  position of the tube. In comparison to the other places, the variation in surface temperature with time is low near the top of the tube.

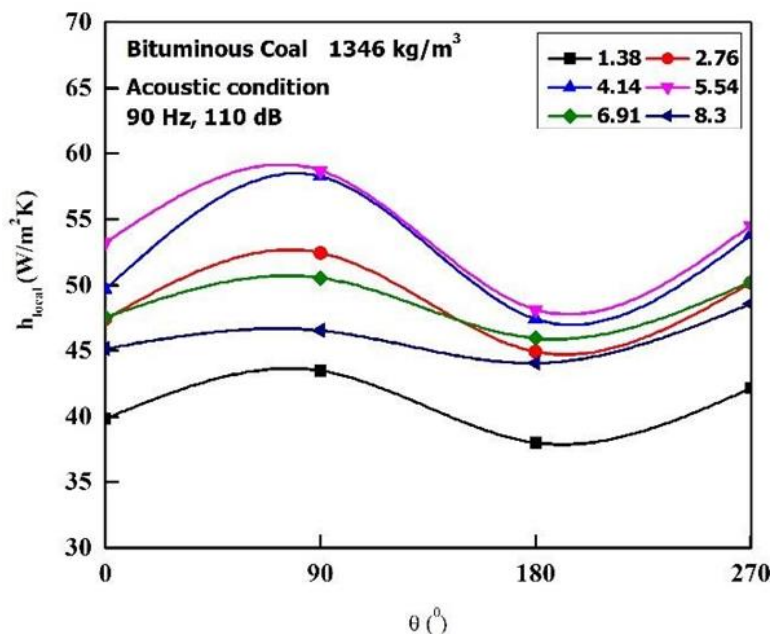


**Figure 7.** Variation in the local convective heat transfer coefficient as a function of angular position around the circumference of the tube for Bituminous Coal,  $Q=8 \text{ W}$ ,  $L/D=1$ , 110 dB, 90 Hz

### 3.5. Average convective heat transfer coefficient with angular position

Figure 9 illustrates the variation in the average heat transfer coefficient for sand under two conditions: with and without the presence of an acoustic field. The data is presented in relation to the excessive air velocity. The observed trend suggests that the average heat transfer coefficient exhibits an increase above 110 dB and extends up to 140 dB. Nevertheless, it is observed that the average heat transfer coefficient experiences a decline once it above the threshold of 140 dB. The acoustic field has a substantial influence on the fluidizing behaviour of ultrafine particles, which has a large effect on the heat transfer coefficient. According to the findings, the average heat transfer coefficient rose as sound pressure and excessive air velocity ratio increased. An average coefficient of heat transfer reached its extreme at 6.6 cm/s and 130 dB-140 dB excessive air velocity and subsequently decreased as air velocity increased. The average heat transfer coefficient was also shown to be dependent on bubble frequency



and packet residence time at the heated surface. The bubble frequency increases as the gas velocity increases, and as a result, amount of time the packet stays on the heated surface is reduced. As a result, the heat transfer coefficient increases. However, as the gas velocity exceeds 6.3 cm/s and the SPL exceeds 140 dB, the packet does not have enough contact time to transmit heat from the heated surface, resulting in reduced heat transfer.

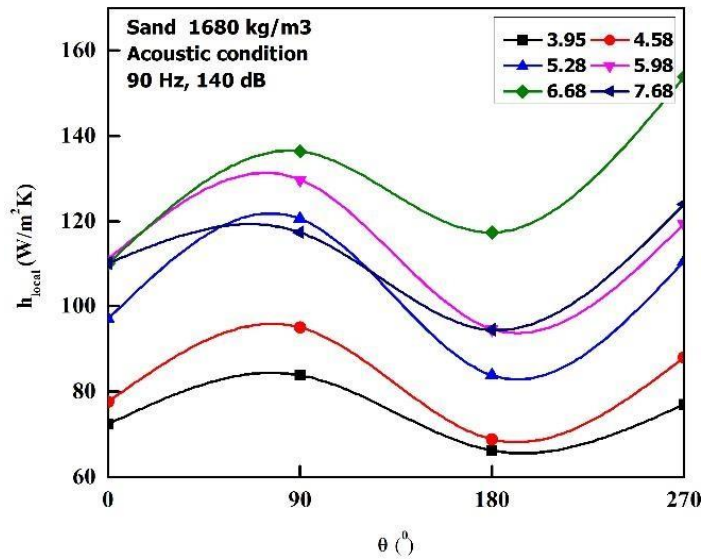


**Figure 8.** Variation of Surface temperature with angular position around the circumference of the tube, Q=8 W, L/D=1, 140dB, 90 Hz

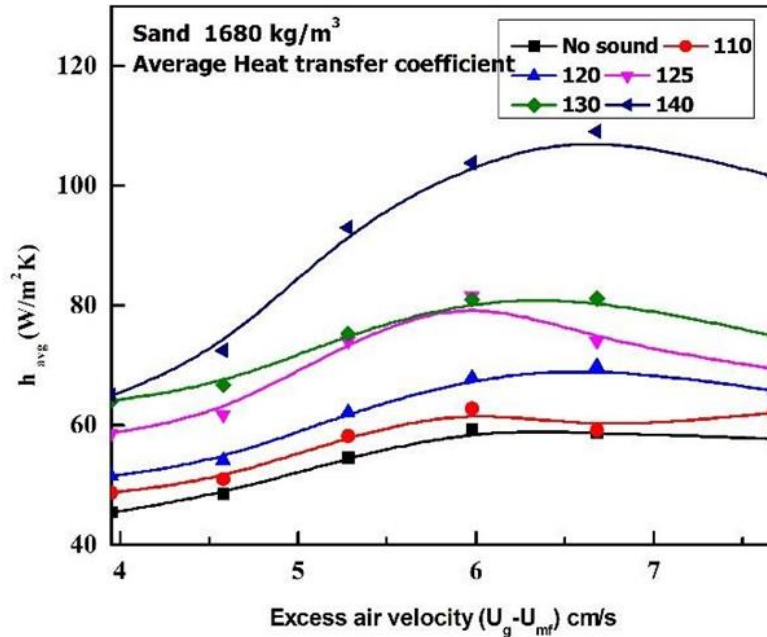


**Figure 9.** Average convective heat transfer coefficient variation for Q=8 W, L/D=1 Sand, and 90 Hz at an angular location along the tube's diameter

### 3.6. Reason for Higher Bed Expansion for Sand

The bed expansion depends upon the emulsion phase porosity, which depends upon the amount of gas dispersed in the solid phase. More gas in the emulsion phase means better gas-to-solid contact, which is measured by an increase in bed expansion. As fluidizing gas flow increased further, gas bypassed the bed in the form of bubbles which gives rise to fluctuation in the pressure and bed height. For similar acoustic circumstances, the



minimum bubbling velocity decreases as density increases. Sound vibrates particles differently depending on particle density. Because sound-induced particle vibrations need less energy for lighter particles such as sand (250  $\mu\text{m}$ ), a relatively modest SPL was sufficient to change the powder structure. Furthermore, as compared to other powders employed in this investigation, the bed expansion was greater.

#### 4. TRANSFER IN A FLUIDIZED BINARY MIXTURE BED WITH SOUND ASSISTANCE

Lignite coal is very hard to fluidize due to severe cohesiveness under all conditions of gas velocities. Channels and cracks were continuously formed even with the application of sound waves. The surface-to-bed heat transfer coefficient was very low due to very poor solid mixing in the bed. Hence it was beneficial to use a binary mixture with specific composition in which the mixture could fluidize properly.

##### 4.1. Mixing and Segregation of Fluidized Binary Mixture

By varying the densities, sizes, and gas velocities of the mixture components, segregation of the particles occurs in the fluidized beds of the binary mixture. It is also conceivable that compounds with varied sizes and comparable densities will segregate to a larger extent than components with varying densities but the same size. Therefore, it is crucial to choose materials that have densities that are about equivalent to those of fine particles. The material with a higher density, known as jetsam, has a tendency to sink, whereas the material with a lower density, known as flotsam, seems to have a trend to float. (Prasad Babu, P.S.T., and Krishnaiah 2017). The degree of segregation was found to vary with the gas flow rate. Higher gas velocities show less segregation in the binary mixture, which displays strong segregation at lower gas velocities. The degree of segregation or mixing in the fluidizing bed also influences the minimum fluidization velocity.

##### 4.2. Fluidization and Heat Transfer of Binary Mixture with And Without Sound Conditions

Coal powder (20  $\mu\text{m}$ ) could not be properly fluidized at all due to severe cohesiveness under all conditions of gas velocities and SPL. Channels and cracks continuously formed even with the application of sound waves. The surface-to-bed heat transfer coefficient was very low due to very poor solid mixing in the bed. Hence, a binary mixture was used with specific composition at which the mixture could be fluidized properly. This resulted in a dramatic increase in the surface-to-bed heat transfer coefficient. The sand was shown to be ineffective in improving the fluidization quality of bituminous coal with a high mass ratio, i.e. for 75% Coal. It was evident that, below the mass concentration of 25% for sand, the bed fluidized with slugging and channelling. It was also discovered that with an increased sand mass percentage, the region of channelling accidents and bubble flow was visible with suitable SPL and frequency adjustments. The quality of fluidization and hence the surface-to-bed heat transfer coefficient were found to be superior for binary mixtures containing 50% or more sand by volume.

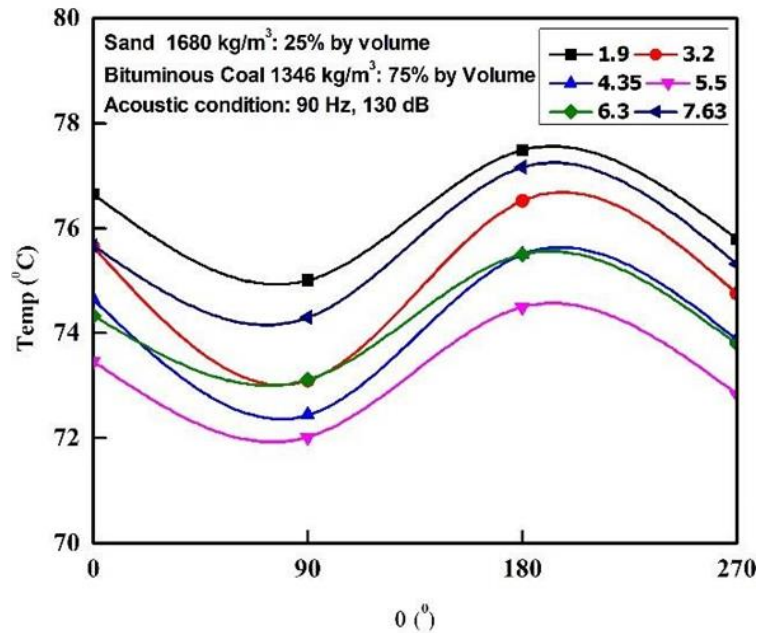
##### 4.3. The Temperature on The Surface and The Angular Position Around the Tube's Circumference

Figure 10 depicts variability in surface temperature at four different angles around the heating tube's circumference. The excessive gas velocity ( $u_g - u_{mf}$ ) varied from 1.9 to 7.63 cm/s for 25% sand - 75% coal. Maximum surface temperature, i.e. 81.48°C were observed at 180° of the tube with 2.97 cm/s, no sound conditions, and reduced with an increase in the excessive gas velocity and SPL. A maximum bed temperature of 64.87 °C was observed at 110 dB SPL and an excessive velocity of gas 4.35 cm/s. Figure 10 shows that the variance of the surface temperature to the angular location is minimal for the top thermocouple ( $\Theta = 180^\circ$ ) for all SPL settings.

##### 4.4. Angular Position ( $\Theta$ ) Vs Local Heat Transfer Coefficient at Excessive Air Velocities

The local coefficient of heat transfer with excessive air velocity ( $u_g - u_{mf}$ ) at various values of  $\Theta$  is depicted in Figure 12. The local heat transfer coefficient exhibited an initial increase when the surplus air velocity increased from 2.2 cm/s to 8.8 cm/s, followed by a subsequent proportional decrease. The local heat transfer magnitude reaches its highest at the lateral edges of the tube, namely at angles of 90 degrees and 270 degrees, while it attains its minimum value at the upper surface of the tube, corresponding to an angle of 180 degrees. It has been noticed

that, Compared to no sound conditions, a binary mixture showed 1.8 times more convective heat transfer coefficient at 6.3 cm/s and 144 dB SPL.



**Figure 10.** Variation of Surface temperature with angular position around the circumference of the tube for 25% sand + 75% Bituminous Coal, Q=8 W, L/D=1, 130dB, (e) 140 dB. (f) 144 dB

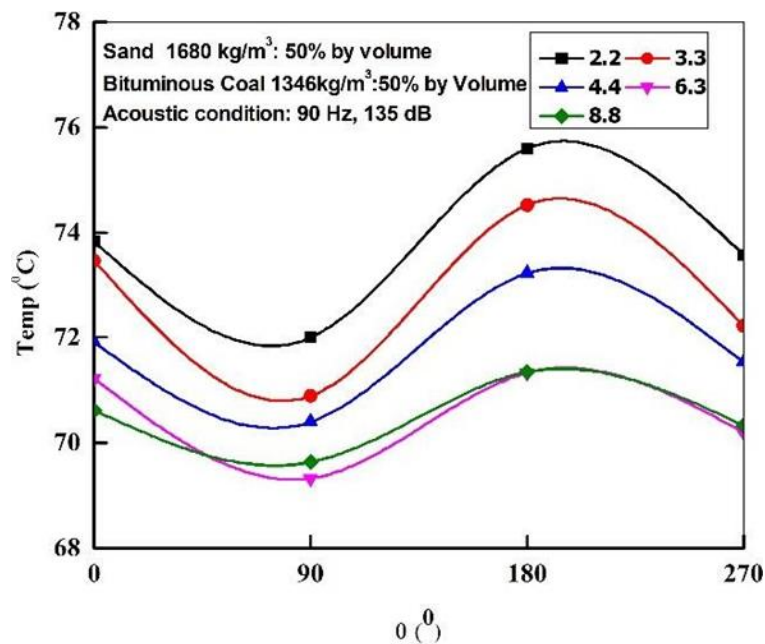
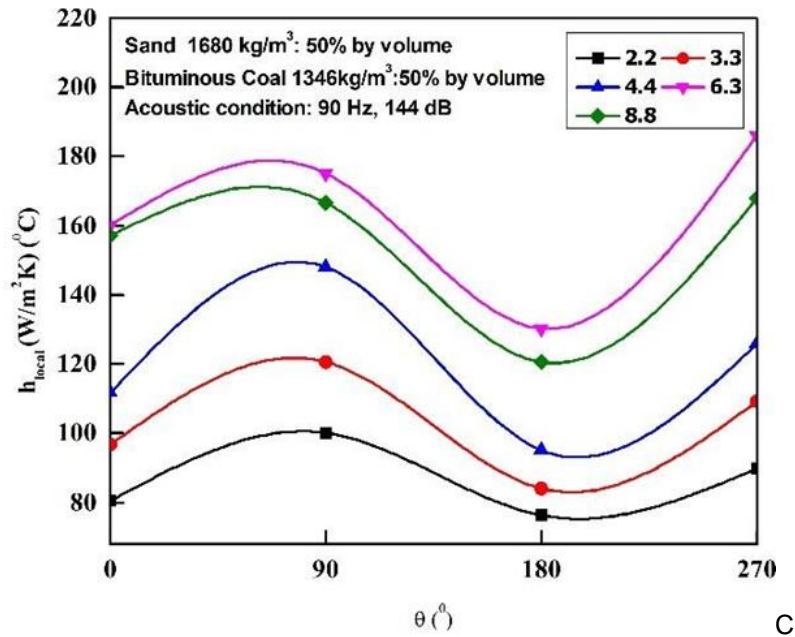


**Figure 11.** Surface temperature changes with angular position around the circumference of a tube containing 50% sand and 50% bituminous coal., Q=8 W, L/D=1, 135 dB, 90 Hz

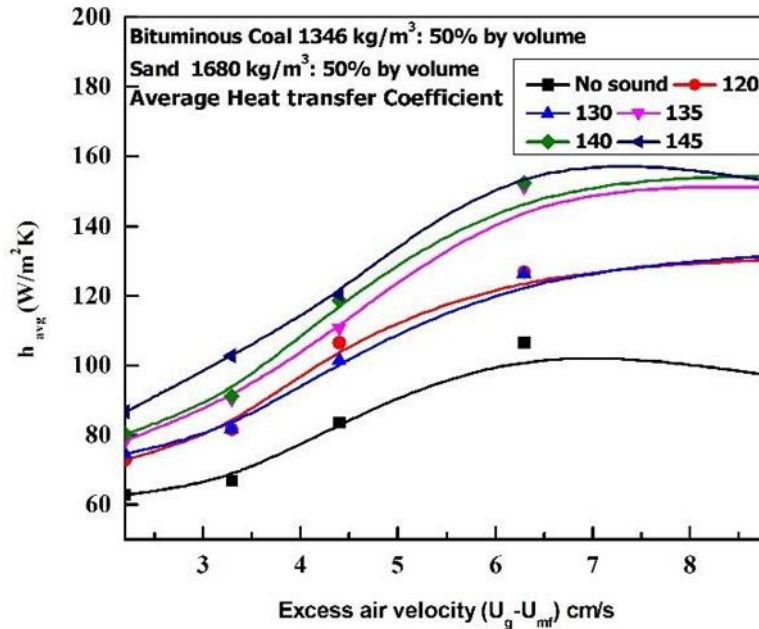
#### 4.5. Average Heat Transfer Coefficient as A Function Of Excessive Air Velocity

Figure 13 depicts how the average heat transfer coefficient varies with excessive air velocity on various SPL. At 6.3 cm/sec, 145 dB, and a binary combination of 50% sand+50% bituminous coal, the greatest average heat transfer coefficient was determined to be 162.93 w/m<sup>2</sup>K. The average heat transfer coefficient had a nearly uniform value across all conditions, provided that the sound intensity remained below 110 dB. However, the values

rapidly rose in the SPL region over 110 dB.



**Fig. 12** Variation of Local convective heat transfer coefficient with angular position around the circumference of the tube for 50% sand + 50% Bituminous Coal,  $Q=8$  W,  $L/D=1$ , 144 dB, 90 Hz



**Figure 13.** Average convective heat transfer coefficient variation with angular location around the tube's diameter for 50% bituminous coal + 50% sand,  $Q=8$  W,  $L/D=1$ , 90 Hz

It was also shown that the average heat transfer coefficient grows monotonically as excessive air velocity increases up to 6.3 cm/s. There was no change in the heat transfer coefficient recorded above that velocity. Figure 14 further showed that the highest heat transfer rates were obtained for a binary combination of 50% sand and 50% bituminous coal.

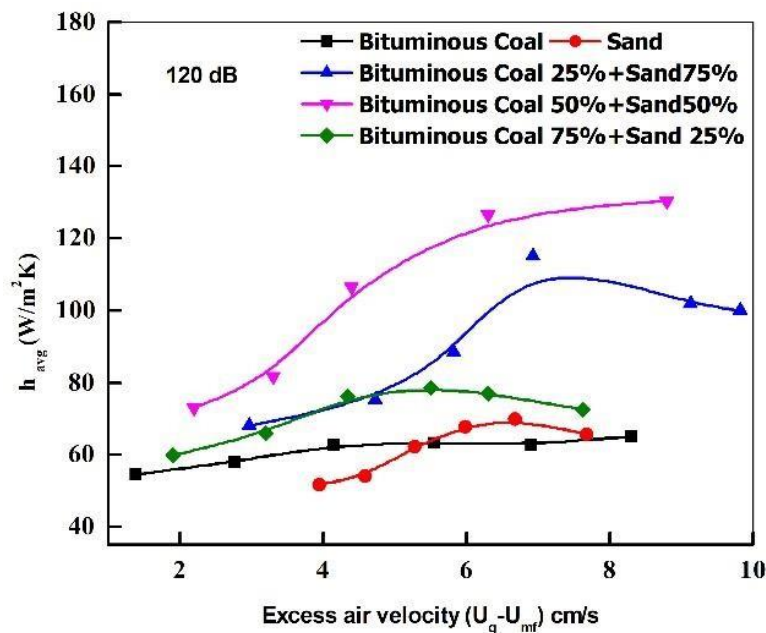


**Figure 14.** Variation of Average convective heat transfer coefficient of binary mixture with the different values of sound intensity for  $Q=8$  W,  $L/D=1$ , 120 dB, 90 Hz

## CONCLUSION

The study focused on exploring heat transfer in a fluidized bed system using a binary mixture of sand and bituminous coal as bed materials. Various parameters such as gas velocities, acoustic frequencies, bed heights, and surface temperatures were considered in the experimental investigation. The key findings are as follows:

- Sound waves with higher sound pressure levels (SPL) at the distributor corresponded to higher SPL values in the fluidized bed column. A selection was made to utilise an acoustic frequency of 90 Hz in order to optimise the sound pressure level (SPL) in the bed.
- The temperature distribution along the tube's diameter was influenced by gas bubbles at the top and material circulation. Increased sound pressure levels resulted in decreased tube temperatures due to greater unpredictability in the fluidizing zone.
- Heat transfer coefficient at the local level was found to be unaffected by changes in air velocity, but it exhibited an increase when gas velocities were higher. This phenomenon can be attributed to the accelerated renewal of particle packets. Heat transfer coefficient reached its maximum value when the surplus air velocity was 5.54 cm/s. Three separate particle motions were detected along the perimeter of the tube. The interface where sliding and mixing motions occur exhibited the highest heat transfer coefficients.
- The average heat transfer coefficient increased with higher sound pressure ratios and excessive air velocities up to a certain point. It reached its peak at an excessive air velocity of 6.6 cm/s and sound pressure levels of 130-140 dB, after which it decreased with further increases in air velocity. Bubble frequency and packet residence time at the heated surface also influenced the heat transfer coefficient.

- The replacement of difficult-to-fluidize lignite coal with a binary mixture of specific composition improved fluidization and surface-to-bed heat transfer coefficient. The binary mixture demonstrated significant enhancement in heat transfer compared to pure coal powder.
- Surface temperature varied with angular position around the tube's circumference, with the maximum temperature observed at 180°. Higher coefficients of convective heat transfer were observed for binary mixture compared to pure coal powder. The local heat transfer coefficient was highest at the sides of the tube (90° and 270°) and lowest at the top surface (180°).
- The mean heat transfer coefficient exhibited variation in response to changes in excessive sound pressure and air velocity level. Highest average heat transfer coefficient was achieved with a binary mixture of 50% sand and 50% bituminous coal under specific conditions.
- The experimental findings suggest that sound assistance can enhance fluidization behavior of binary mixtures. Sound assistance mitigates the effect of particle-particle heat transfer due to the space between particles during fluidization. Combining group C particles (e.g., coal) with group B particles (e.g., silica sand) improves heat transmission outcomes.
- The application of assisting techniques, generating vibrations within the bed at specific amplitudes and frequencies, can prevent bubbling during the fluidization of the bituminous coal bed.
- The study indicates that if particle packet movement controls heat transfer, the variation in the heat transfer coefficient at the top of the tube may be minimal, as solid particles are affected by bubbles.

### Acknowledgement

The authors express their gratitude to the Department of Mechanical Engineering, School of Engineering, OP Jindal University Raigarh, India for providing the research grant.

### Conflict of Interest

There is no conflict of interest.

## REFERENCES

- [1] Abdelmotalib, Hamada M., Mahmoud A. M. Youssef, Ali A. Hassan, Suk Bum Youn, and Ik Tae Im. 2015. "Heat Transfer Process in Gas-Solid Fluidized Bed Combustors: A Review." *International Journal of Heat and Mass Transfer* 89:567–75. doi: 10.1016/j.ijheatmasstransfer.2015.05.085.
- [2] Al-Ghurabi, Ebrahim H., Syed Sadiq Ali, Sulaiman M. Alfadul, Mohammed Shahabuddin, and Mohammad Asif. 2019. "Experimental Investigation of Fluidized Bed Dynamics under Resonant Frequency of Sound Waves." *Advanced Powder Technology* 30(11):2812–22. doi: 10.1016/j.apt.2019.08.028.
- [3] Ali, Syed Sadiq, Ebrahim H. Al-ghurabi, Abdelhamid Ajbar, Yahya A. Mohammed, Mourad Boumaza, and Mohammad Asif. 2016. "Effect of Frequency on Pulsed Fluidized Beds of Ultrafine Powders." *Hindawi Publishing Corporation Journal of Nanomaterials* 1–12.
- [4] Ali, Syed Sadiq, and Mohammad Asif. 2017. "Effect of Particle Mixing on the Hydrodynamics of Fluidized Bed of Nanoparticles." *Powder Technology* 310:234–40. doi: 10.1016/j.powtec.2017.01.041.
- [5] Bai, Yong, and Hui Si. 2020. "Experimental Study on Fluidization, Mixing and Separation Characteristics of Binary Mixtures of Particles in a Cold Fluidized Bed for Biomass Fast Pyrolysis." *Chemical Engineering and Processing - Process Intensification* 153:107936. doi: 10.1016/j.cep.2020.107936.
- [6] Chang, Jian, Shuqing Yang, and Kai Zhang. 2011. "A Particle-to-Particle Heat Transfer Model for Dense Gas-Solid Fluidized Bed of Binary Mixture." *Chemical Engineering Research and Design* 89(7):894–903. doi: 10.1016/j.cherd.2010.08.004.
- [7] Chirone, Roberto, Federica Raganati, Paola Ammendola, Diego Barletta, Paola Lettieri, and Massimo Poletto. 2018. "A Comparison between Interparticle Forces Estimated with Direct Powder Shear Testing and with Sound Assisted Fluidization." *Powder Technology* 323:1–7. doi: 10.1016/j.powtec.2017.09.038.
- [8] Dong, Pengfei, Zhanyong Li, Xinyuan Gao, Zhonghua Wu, and Zechun Zheng. 2013. "Evaluation of Hydrodynamic Behavior of a Fluidized

- Bed Dryer by Analysis of Pressure Fluctuation." *Drying Technology* 31(10):1170–76. doi: 10.1080/07373937.2013.781621.
- [9] Freitas, T. M., L. S. Arrieche, D. C. Ribeiro, D. Gidaspow, and M. S. Bacelos. 2017. "CFD Analysis of Fluidized Beds Using Wastes from Post-Consumer Carton Packaging." *Chemical Engineering and Processing: Process Intensification* 111:89–100. doi: 10.1016/j.cep.2016.12.002.
- [10] Gabhane, Mohitkumar G., Siddharth S. Chakrabarti, and Uday S. Wankhede. 2021. "Parameters Influencing the Performance of Fluidized Bed: A Review on Thermo-Hydraulic Properties." *Energy Sources, Part A: Recovery, Utilization and Environmental Effects* 00(00):1–34. doi: 10.1080/15567036.2021.1971336.
- [11] Gabhane, Mohitkumar G., and U. S. Wankhede. 2017. "Developments in Fluidized Bed Technology." Pp. 1–6 in *International conference on Advances in Thermal Systems, Materials and Design Engineering (ATSMDE2017)*.
- [12] Geldart, D. 1973. "Types of Gas Fluidization." *Powder Technology* 7:285–92.
- [13] Gohel, Mukesh, Lalji Baldaniya, and Bhavesh Subhashchandra Barot. 2007. "Fluidized Bed Systems : A Review Pharmainfo . Net Fluidized Bed Systems : A Review." (January).
- [14] Hamam, Mohamed, M. Tawfik, Mohamed Refaat, and Hamada Mohamed. 2020. "Heat Transfer and Hydrodynamics of Particles Mixture in Swirling Fluidized Bed." *International Journal of Thermal Sciences* 147(September 2019):106134. doi: 10.1016/j.ijthermalsci.2019.106134.
- [15] Hamidipour, Mohsen, Navid Mostoufi, Rahmat Sotudeh-Gharebagh, and Jamal Chaouki. 2005.
- [16] "Experimental Investigation of Particle Contact Time at the Wall of Gas Fluidized Beds." *Chemical Engineering Science* 60(15):4349–57. doi: 10.1016/j.ces.2005.03.006.
- [17] Han, Mengqi. 2015. "Characterization of Fine Particle Fluidization." Western university.
- [18] Kang, Dong Hyun, Sung Il Kim, Won Pyo Chun, and Dong Hyun Lee. 2017. "Drying Characteristics of Fine Powders in an Inert Medium Circulating Fluidized Bed with Binary Inert Media." *Journal of Industrial and Engineering Chemistry* 45:266–76. doi: 10.1016/j.jiec.2016.09.034.
- [19] Kim, Jun Young, Jong Wook Bae, John R. Grace, Norman Epstein, Dong Hyun Lee, and D. Hyun. 2017. "Horizontal Immersed Heater-to-Bed Heat Transfer with Layer Inversion in Gas-Liquid- Solid Fluidized Beds of Binary Solids." *Chemical Engineering Science* 170:502–7. doi: 10.1016/j.ces.2017.01.007.
- [20] Leckner, Bo, Pal Szentannai, and Franz Winter. 2011. "Scale-up of Fluidized-Bed Combustion-a Review." *Fuel* 90(10):2951–64. doi: 10.1016/j.fuel.2011.04.038.
- [21] Nimvari, Mohsen Isaac, Reza Zarghami, and Davood Rashtchian. 2020. "Experimental Investigation of Bubble Behavior in Gas-Solid Fluidized Bed." *Advanced Powder Technology* 31(7):2680–88. doi: 10.1016/j.apt.2020.04.031.
- [22] Prasad Babu, M., Sai P.S.T., and K. Krishnaiah. 2017. "Continuous Segregation of Binary Heterogeneous Solids in Fluidized Beds." *Particuology* 35:93–100. doi: 10.1016/j.partic.2017.05.004.
- [23] Raganati, Federica, Riccardo Chirone, and Paola Ammendola. 2017. "Effect of Temperature on Fluidization of Geldart's Group A and C Powders: Role of Interparticle Forces." *Industrial and Engineering Chemistry Research* 56(44):12811–21. doi: 10.1021/acs.iecr.7b03270.
- [24] Shrestha, S., S. B. Kuang, A. B. Yu, and Z. Y. Zhou. 2020. "Effect of van Der Waals Force on Bubble Dynamics in Bubbling Fluidized Beds of Ellipsoidal Particles." *Chemical Engineering Science* 212:111343. doi: 10.1016/j.ces.2019.115343.
- [25] Tang, Zhidong, Peng Gao, Yongsheng Sun, and Yuexin Han. 2019. "Experimental Study on Fluidization Characteristics of Different-Sized Particles in a U-Type Reduction Chamber." *Advanced Powder Technology* 30(10):2430–39. doi: 10.1016/j.apt.2019.07.028.
- [26] Vaidya, V. B., R. L. Sonolikar, and S. B. Thombre. 2013. "Heat Transfer Study of Binary Mixture of Group B Particles in the Gas – Solid Fluidized Bed Using Acoustic Field." *International Journal of Mechanics and Thermodynamics* 4(1):11–19.
- [27] Valverde, Jose Manuel, and Antonio Castellanos. 2008. "Fluidization of Nanoparticles : A Simple Equation for Estimating the Size of Agglomerates." 140:296–304. doi: 10.1016/j.cej.2007.09.032.
- [28] Wang, Dengjia, Jin Liu, Yanfeng Liu, Yingying Wang, Bojia Li, and Jiaping Liu. 2020. "Evaluation of the Performance of an Improved Solar Air Heater with 'S' Shaped Ribs with Gap." *Solar Energy* 195:89–101. doi: 10.1016/j.solener.2019.11.034.
- [29] Wankhede, Uday, and Ram Sonolikar. 2017. "Experimental Analysis and Computational Fluid Dynamics Simulations for Heat Transfer in Sound Assisted Fluidized Bed of Fine Powders." *Thermal Science* 21(5):1953–63. doi: 10.2298/TSC1150208124W.
- [30] Wey, Ming-yen, Chiou-liang Lin, and Shr-da You. 2007. "Fluidized Behavior and Heat Transfer in a Bubbling Fluidized Bed Incinerator." *Journal of Environment, Engineering and Management* 17(3):169–75.
- [31] Xiang, Jie, Qinghai Li, Zhongchao Tan, and Yanguo Zhang. 2017. "Characterization of the Flow in a Gas-Solid Bubbling Fluidized Bed by Pressure Fluctuation." *Chemical Engineering Science* 174:93–103. doi: 10.1016/j.ces.2017.09.001.

DOI: <https://doi.org/10.15379/ijmst.v10i5.2560>

This is an open access article licensed under the terms of the Creative Commons Attribution Non-Commercial License (<http://creativecommons.org/licenses/by-nc/3.0/>), which permits unrestricted, non-commercial use, distribution and reproduction in any medium, provided the work is properly cited.